Binaural active noise control using parametric array loudspeakers

Kihiro Tanaka[a], Chuang Shi[a,*], Yoshinobu Kajikawa[a]

[a]*Department of Electrical and Electronic Engineering, Kansai University, Osaka, Japan*

Abstract

This paper reports the binaural active noise control (ANC) system developed to deal with factory noise. The control points are located in the vicinity of the left and right ears of a worker sitting along the production line. Due to the complicated safety requirements in the factory, secondary sources and error microphones are not allowed to be placed near the worker. Therefore, the proposed ANC system employs the feedforward structure and adopts the parametric array loudspeakers (PALs) as the secondary sources. The PAL is a type of directional loudspeaker that generates a much narrower sound field as compared to the conventional loudspeaker. Once the proposed ANC system has been trained offline, the error microphones can be removed. The performance of the binaural ANC system is successfully demonstrated based on a digital signal processor (DSP) implementation.

Keywords: Feedforward active noise control, Factory noise, Parametric array loudspeaker, Crosstalk

*Corresponding Author's Email: r148005@kansai-u.ac.jp

1. Introduction

In factories, workers suffer from noise induced hearing loss. They sit along the production line and are exposed to the noise generated by manufacturing equipment for prolonged hours. Protective measures are urgently needed to solve this problem. Since verbal communication may be hindered by passive noise control, ANC seems to be the most feasible solution [1]. In an ANC system, the noise source is called the primary source. The secondary source, *a.k.a.* the control source, transmits an anti-noise wave with the equaling amplitude and opposite phase of the noise wave. Based on the superposition principle of sound waves, cancellation of the noise wave can be achieved at the control point, where the error microphone is set up to make the ANC system a closed loop control [2].

There are two basic structures of an ANC system [3]. They are the feedforward and feedback ANC systems. The feedforward ANC system requires an additional reference microphone or sensor to obtain an early observation of the noise wave, while the feedback ANC system computes an estimation of the noise wave internally. If the secondary source and error microphone are placed far from the control point, the feedback ANC system can fail to function. In contrast, the feedforward ANC system can be trained offline to carry out the fixed coefficient implementation [4]. In the fixed coefficient ANC system, the error microphone is removed while the reference microphone continues to track the noise wave.

Usually, the single-channel ANC system uses one secondary source and targets only one control point. When the secondary source is omni-directional, noise reduction is achieved at the control point, but spillover of the anti-noise

wave leads to increased noise levels in other areas [5]. For the same reason, when the single-channel ANC system is applied to target more than one control point, the overall noise reduction performance is often unstable. Alternatively, the dual-channel ANC system uses two secondary sources. Each of the secondary source is principally in charge of one control point. When the secondary sources are omni-directional, crosstalk becomes an unavoidable problem and brings extra computational cost in the implementation, on top of the spillover problem [6]. Therefore, there are advantages of using directional loudspeakers as the secondary sources in ANC systems.

The PAL is a type of directional loudspeaker that makes use of the nonlinear acoustic effect to generate an audio beam from an ultrasonic beam [7]. In literatures, Hansen *et al.* were the first to investigate the feasibility of using the PAL as the secondary source [8, 9]. The preliminary results were negative at very low frequencies, where the conventional ANC system was recognized to be the most efficient. Nevertheless, there have been an increasing number of successful attempts on using the PAL as the secondary source [10]. They have been applied to the midrange and upper midrange bands, such as from 0.5 to 2.5 kHz [11, 12, 13].

Among those successful attempts, Tanaka and his colleagues explored many unique features of the PAL that may improve the conventional ANC system [14]. For example, they used the reflected audio beam of the PAL to transmit the anti-noise wave in order for the control point to be invisible from the secondary source [15]. A steerable PAL that was implemented based on the phased array of ultrasonic transducers was applied in the ANC system targeting a moving control point [16]. Moreover, a curved-type PAL was

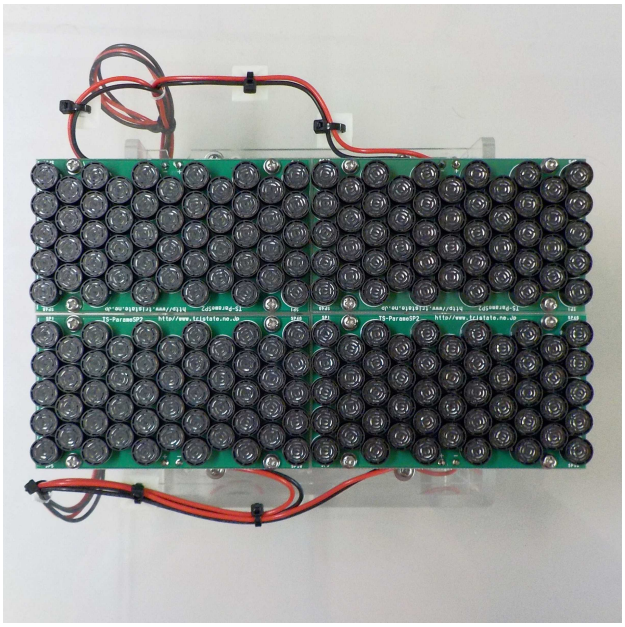

Figure 1: A picture of the PAL.

built up to achieve global noise reduction by manipulating the focal point of the curved-type PAL to be located at the exact location of a monopole noise source [17].

This paper reports the binaural ANC system developed to create quiet zones in the vicinity of the left and right ears of a worker in the factory. According to the complicated safety requirements in the factory, secondary sources and error microphones are not allowed to be placed near the worker. Hence, it is reasonable for the binaural ANC system to employ the feed-forward structure and adopt the parametric array loudspeakers (PALs) as the secondary sources. The PAL used in this paper is shown in Fig. 1, of which the dimension is 20 cm in width and 11 cm in height. It is made up of four units of Tristate K-02617. The audio bandwidth ranges from 0.4 to

5 kHz. Furthermore, the fixed coefficient implementation is also essential for the binaural ANC system to get rid of the error microphones, under the consideration that the worker is able to adjust his or her position to rest in the quiet zones.

Therefore, this paper is organized as follows. In the next section, the performance of the single-channel ANC system that targets two control points is demonstrated using one PAL. In Section 3, the dual-channel ANC system is examined with and without the crosstalk secondary path models when two PALs are used as the secondary sources. Furthermore, the performance of the fixed coefficient ANC system is presented to prove the feasibility of the binaural ANC system when there are no secondary sources and error microphones placed near the control points.

2. Single-channel ANC system using the PAL

The experimental setup of the single-channel ANC system is shown in Fig. 2. The factory noise sample shown in Fig. 3(a) is played back by an omnidirectional loudspeaker to provide the noise source. There are periodical impulsive components generated by the packaging machine. The ambient noise in the factory is shown in Fig. 3(b), which is used to provide another noise source in the latter part of this paper. The reference microphone is placed close to the noise source. The PAL shown in Fig. 1 is used as the secondary source. The head and torso simulator (HATS) mimics the worker in a stationary position. The left and right ears of the HATS are used as the error microphones. The distances from the noise source and PAL to the error microphones are roughly 200 cm and 150 cm, respectively.

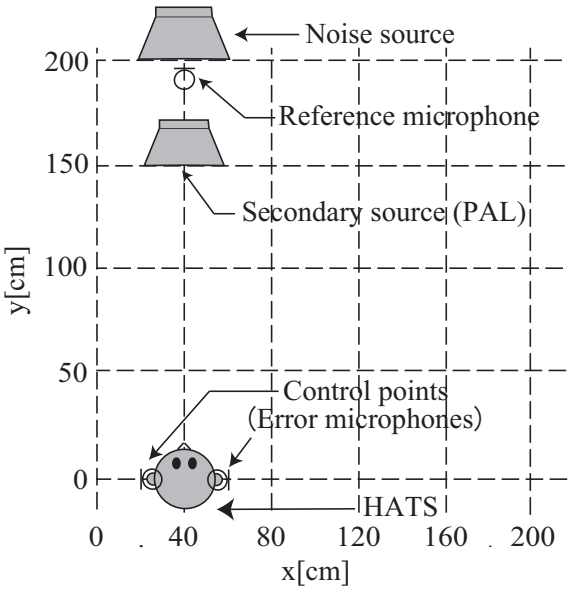

Figure 2: Experimental setup of the single-channel ANC system.

The structure of the single-channel ANC system is shown in Fig. 4, where $\mathbf{u}(n)$ is the reference signal vector; $d_1(n)$ and $d_2(n)$ are the noise signals; $y(n)$ is the anti-noise signal; $e_1(n)$ and $e_2(n)$ are the error signals picked up by the error microphones. The error signals are expressed as

$$\begin{aligned} e_m(n) &= d_m(n) - y_m(n) \\ &= d_m(n) - \mathbf{s}_m(n) * [\mathbf{w}^T(n)\mathbf{u}(n)], \end{aligned} \tag{1}$$

where $m = 1$ or 2 indicates the error microphone index; $\mathbf{s}_m(n)$ is the impulse response of the secondary path $S_m(z)$; and $\mathbf{w}(n)$ is the coefficient vector of the noise control filter.

Since the instantaneous squared error is computed as

$$e^2(n) = e_1^2(n) + e_2^2(n), \tag{2}$$

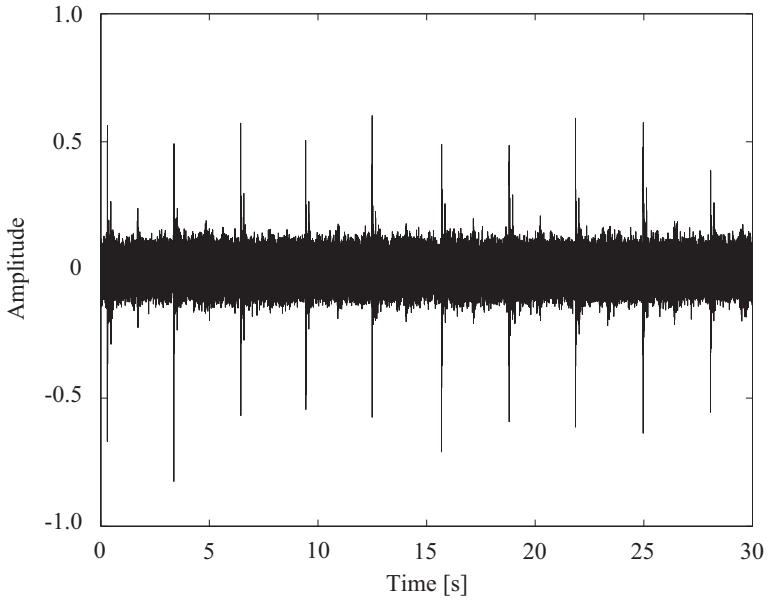

(a) Periodical impulsive noise

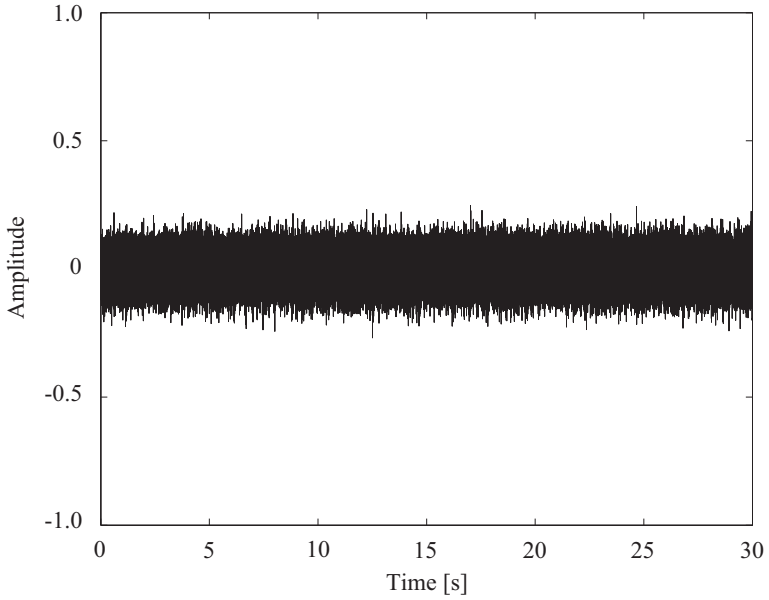

(b) Ambient noise

Figure 3: Noise samples recorded in the factory.

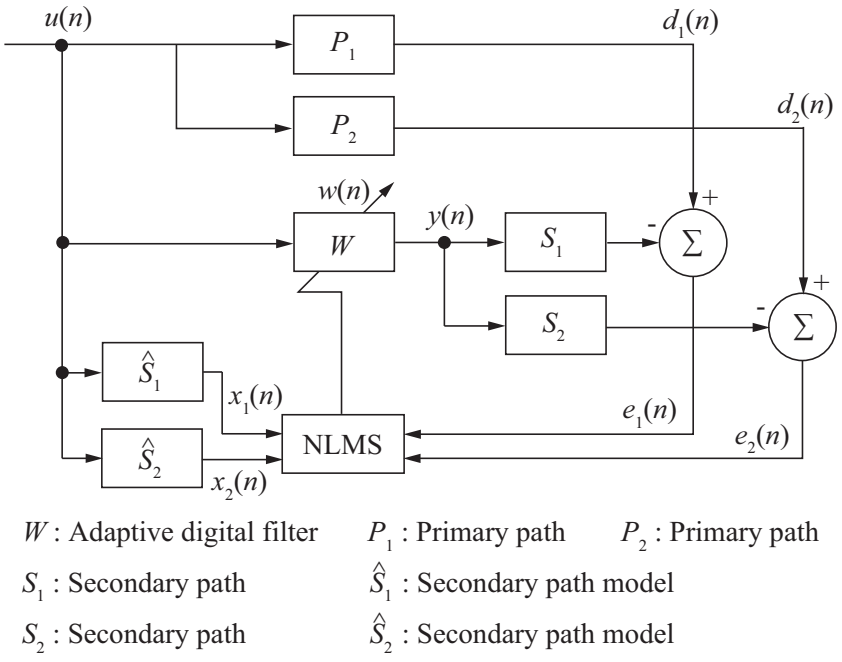

Figure 4: FxLMS structure of the single-channel ANC system.

the normalized Filtered-x Least Mean Squares (FxLMS) algorithm is available to update $\mathbf{w}(n)$ as

$$\mathbf{w}(n+1) = \mathbf{w}(n) + \sum_{m=1}^{2} \frac{\alpha}{\beta + ||\mathbf{x}_m(n)||^2} \mathbf{x}_m(n) e_m(n), \tag{3}$$

where $\mathbf{x}_m(n) = \hat{\mathbf{s}}_m(n) * \mathbf{u}(n)$ is the filtered reference signal vector; and $\hat{\mathbf{s}}_m(n)$ is the impulse response of the secondary path model $\hat{S}_m(z)$. Let L and N denote the tap lengths of $\mathbf{w}(n)$ and $\hat{\mathbf{s}}_m(n)$, respectively. The computational cost of the single-channel ANC system includes 2 divisions, $3L + 2N + 6$ multiplications, and $3L + 2N + 1$ additions in every iteration, since each denominator in (3) can be efficiently calculated using only 2 multiplications and 2 additions [18].

In the experiment, the sampling frequency is 12 kHz. The tap lengths are

$L = 400$ and $N = 200$. The step size is $\alpha = 1.0 \times 10^{-3}$. The regularization parameter $\beta = 1.0 \times 10^{-6}$ is introduced to avoid numerical difficulties when $||\mathbf{x}_m(n)||^2$ is too small. The implementation is carried out on the DSP starter kit (TMS320C6713, Texas Instruments). Four channels of digital-to-analog conversion and eight channels of analog-to-digital conversion are provided by the interface board (DSK6713IFA, Hiratsuka Engineering). The anti-aliasing filters (MSPAMP800, Hiratsuka Engineering) are set to have the same cut-off frequency at 2.5 kHz. In the rest of this paper, the parameters remain the same if not specifically mentioned.

Figure 5 shows the experiment results of the single-channel ANC system. The single-channel ANC system is stably effective from 1 to 2.5 kHz at both the left and right ears of the HATS. However, the noise reduction performance is sensitive to the position of the HATS. The experimental setup has been determined by the trial and error manner in our experiments.

3. Dual-channel ANC system using two PALs

The dual-channel ANC system uses two PALs as the secondary sources. Each of them corresponds to one ear of the HATS. Based on a previous study, the experimental setup shown in Fig. 6 provides the optimized performance [19]. The structure of the dual-channel ANC system is shown in Fig. 7, where $y_1(n)$ and $y_2(n)$ are the anti-noise signals; $S_{11}(z)$ and $S_{22}(z)$ are the secondary paths; $S_{21}(z)$ and $S_{12}(z)$ are the crosstalk secondary paths; $\hat{S}_{11}(z)$ and $\hat{S}_{22}(z)$ are the secondary path models; $\hat{S}_{21}(z)$ and $\hat{S}_{12}(z)$ are the crosstalk secondary path models.

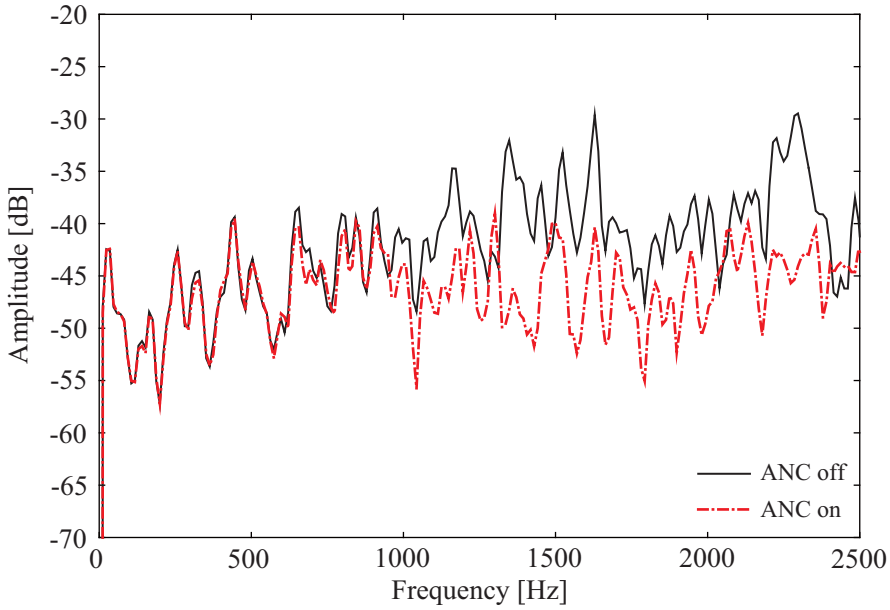

(a) Left ear

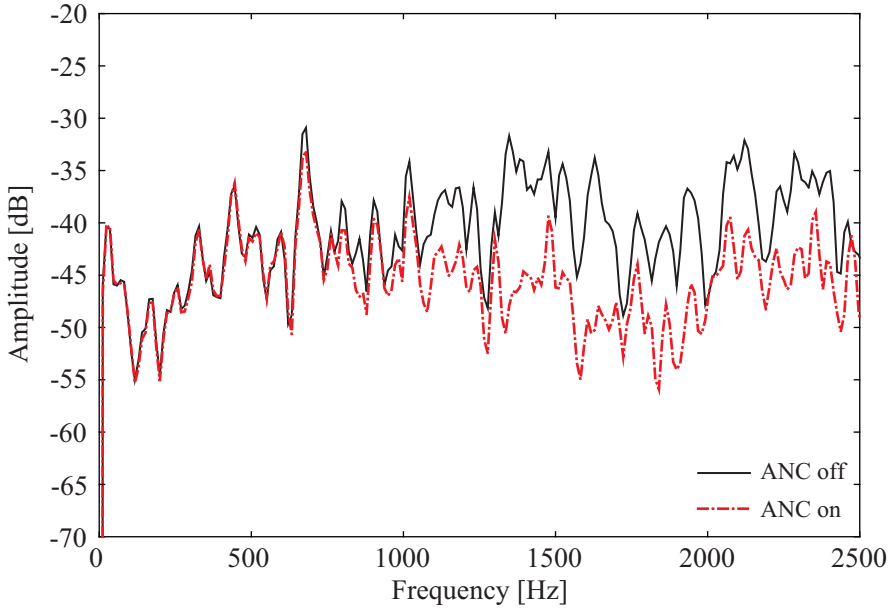

(b) Right ear

Figure 5: Experiment results of the single-channel ANC system that achieves 5.0 dB and 5.6 dB noise reductions at the left and right ears, respectively.

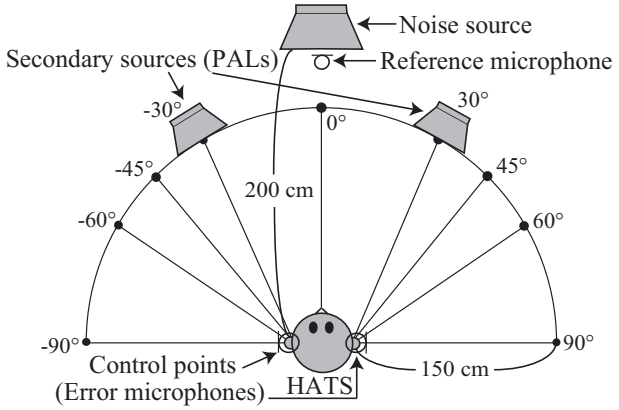

Figure 6: Experimental setup of the dual-channel ANC system.

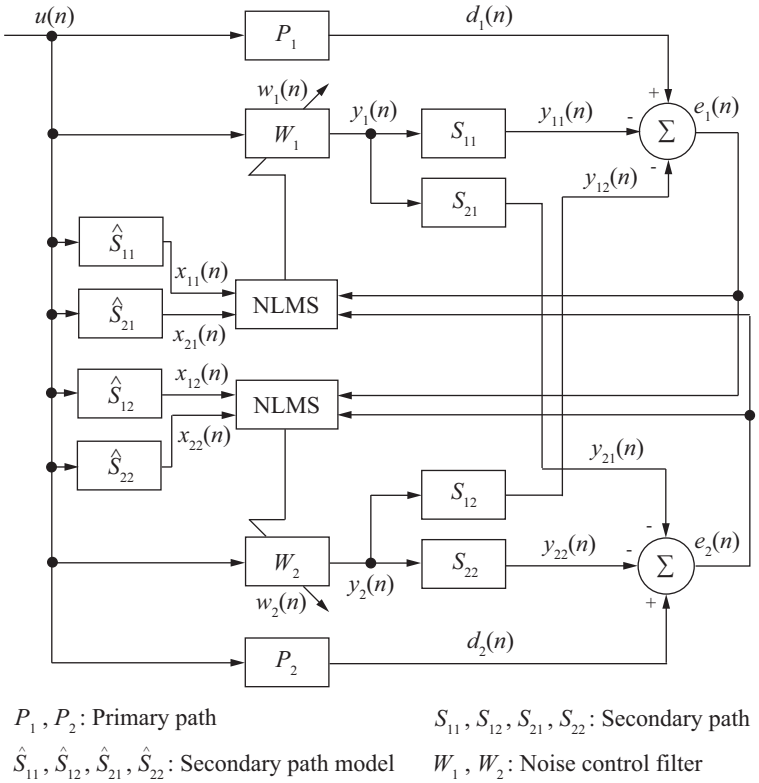

Figure 7: Structure of the dual-channel ANC system.

The error signals $e_1(n)$ and $e_2(n)$ are expressed as

$$\begin{aligned} e_1(n) &= d_1(n) - y_{11}(n) - y_{12}(n) \\ &= d_1(n) - \mathbf{s}_{11}(n) * [\mathbf{w}_1^T(n)\mathbf{u}(n)] - \mathbf{s}_{12}(n) * [\mathbf{w}_2^T(n)\mathbf{u}(n)] \end{aligned} \tag{4}$$

and

$$\begin{aligned} e_2(n) &= d_2(n) - y_{22}(n) - y_{21}(n) \\ &= d_2(n) - \mathbf{s}_{22}(n) * [\mathbf{w}_2^T(n)\mathbf{u}(n)] - \mathbf{s}_{21}(n) * [\mathbf{w}_1^T(n)\mathbf{u}(n)], \end{aligned} \tag{5}$$

where $\mathbf{s}_{11}(n)$, $\mathbf{s}_{12}(n)$, $\mathbf{s}_{22}(n)$ and $\mathbf{s}_{21}(n)$ are the impulse responses of $S_{11}(z)$, $S_{12}(z)$, $S_{22}(z)$ and $S_{21}(z)$, respectively.

Similar to the single-channel ANC system, the normalized FxLMS algorithm is applied in the dual-channel ANC system as

$$\mathbf{w}_k(n+1) = \mathbf{w}_k(n) + \sum_{m=1}^{2} \frac{\alpha}{\beta + ||\mathbf{x}_{mk}(n)||^2} \mathbf{x}_{mk}(n) e_m(n), \tag{6}$$

where $k = 1$ or 2 indicates the secondary source index; $\mathbf{w}_k(n)$ is the updating coefficient vector of the noise control filter; $\mathbf{x}_{mk}(n) = \mathbf{s}_{mk}(n) * \mathbf{u}(n)$ is the filtered reference signal vector. If the secondary path models and crosstalk secondary path models have the same tap length N, each channel of the dual-channel ANC system results in the same computation cost of the single-channel ANC system in the previous section. Hence, the computation cost of the dual-channel ANC system is doubled to 4 divisions, $6L + 4N + 12$ multiplications, and $6L + 4N + 2$ additions in every iteration.

The PALs have such a narrow directivity that crosstalk is not significant between PALs, and the crosstalk secondary path models can thus be removed.

By doing so, the dual-channel ANC system is decoupled into two single-channel ANC systems that consist of one secondary source and one error microphone. The normalized FxLMS algorithm is applied in each channel as

$$\mathbf{w}_k(n+1) = \mathbf{w}_k(n) + \frac{\alpha}{\beta + ||\mathbf{x}_{kk}(n)||^2}\mathbf{x}_{kk}(n)e_k(n). \tag{7}$$

Therefore, the computational cost of the dual-channel ANC system is reduced to 2 divisions, $4L + 2N + 6$ multiplications and $4L + 2N$ additions in every iteration.

The experiment results of the dual-channel ANC system are shown in Fig. 8. There are two significant improvements as compared to the single-channel ANC system. Firstly, the dual-channel ANC system is effective from 0.5 to 2.5 kHz at the left and right ears of the HATS. Secondly, the noise reduction performance is notably improved, with the exception near 2 kHz. Around 2 kHz, the noise level is increased after the dual-channel ANC system is turned on. This may be contributed by the nonlinear distortion of the PAL. When the crosstalk secondary path models are removed, the performance of the dual-channel ANC system is not compromised, while the computational cost is reduced. Advantages of using directional loudspeakers as the secondary sources are hence demonstrated.

3.1. Fixed coefficient implementation

The offline training is of importance to the binaural ANC system proposed in this paper. The ultimate goal is to implement the binaural ANC system in the factory with no secondary sources and error microphones placed near the worker. After the dual-channel ANC system is turned on for 30 seconds, the coefficients of the noise control filters have been converged. They are saved in

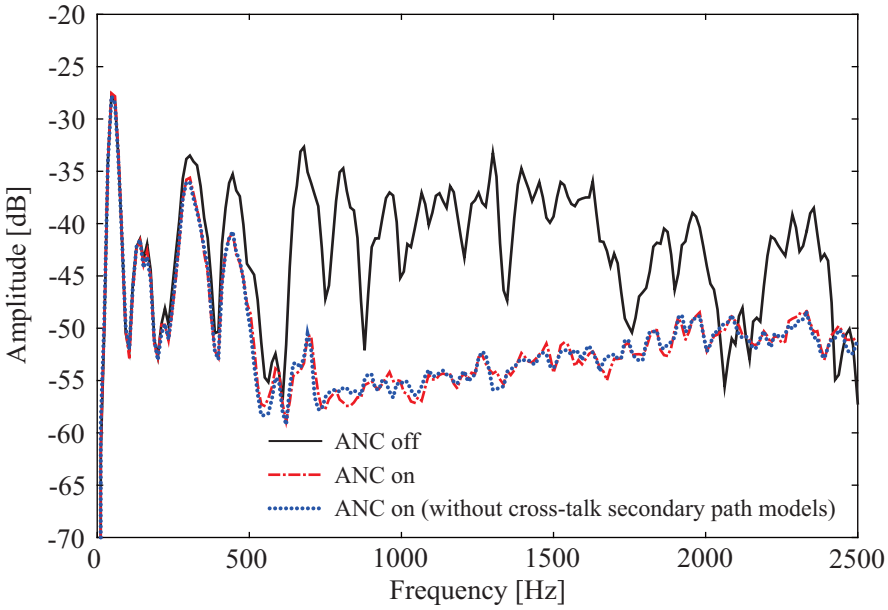

(a) Left ear

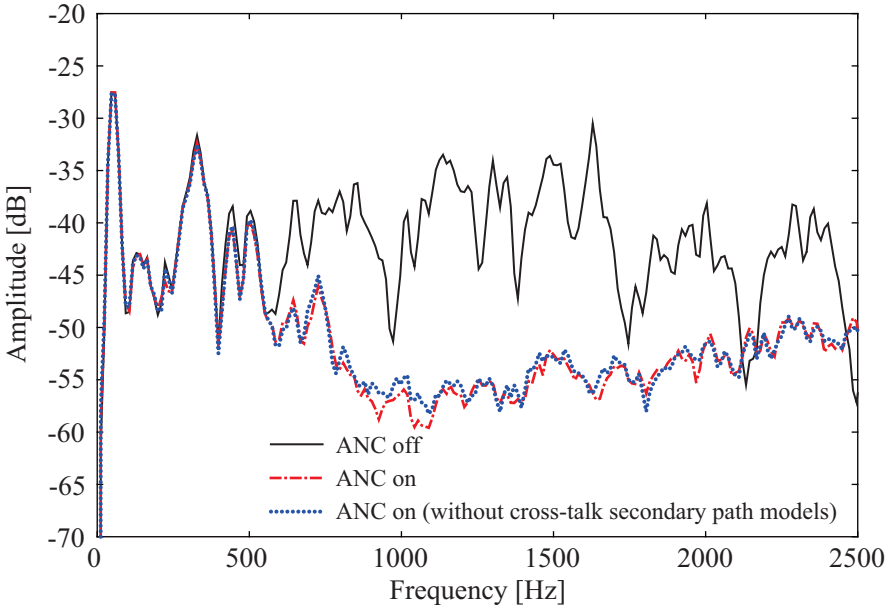

(b) Right ear

Figure 8: Experiment results of the dual-channel ANC system that achieves 10.4 dB and 11.6 dB noise reductions at the left and right ears, respectively.

the memory and then adopted in the fixed coefficient ANC system [20]. The computational cost of the fixed coefficient ANC system is contributed by the two noise control filters, which in totality is counted as $2L$ multiplications and $2L-2$ additions in every iteration.

The experiment results of the fixed coefficient dual-channel ANC system are shown in Fig. 9. The dual-channel ANC system achieves good noise reduction performance even though the crosstalk secondary path models are removed. The noise reduction performance of the fixed coefficient ANC system is reduced due to the perturbation of the room environment. However, as compared to Fig. 5, the fixed coefficient ANC system is still more efficient than the single-channel ANC system. The assumptions behind the fixed coefficient ANC system are the unchanging primary and secondary paths, which are generally valid in the food or pharmaceutical factory, because its temperature and relative humidity are maintained at constant levels. Even though there may be small changes in the quiet zones, workers are still able to adjust their bodies to find the most comfortable positions. Offline training can be arranged at night if any worker reports there is no noise reduction during working hours.

3.2. Case study of two noise sources

Furthermore, we discuss the effect of two noise sources on the performance of the dual-channel ANC system. The experimental setup is shown in Fig. 10, where two noise sources are located at $\pm 30^{\circ}$. Different noise samples, as shown in Figs. 3(a) and 3(b), are played back by separate omnidirectional loudspeakers. The distance from one noise source to the nearer error microphone is kept at 200 cm. In order to deal with two noise sources,

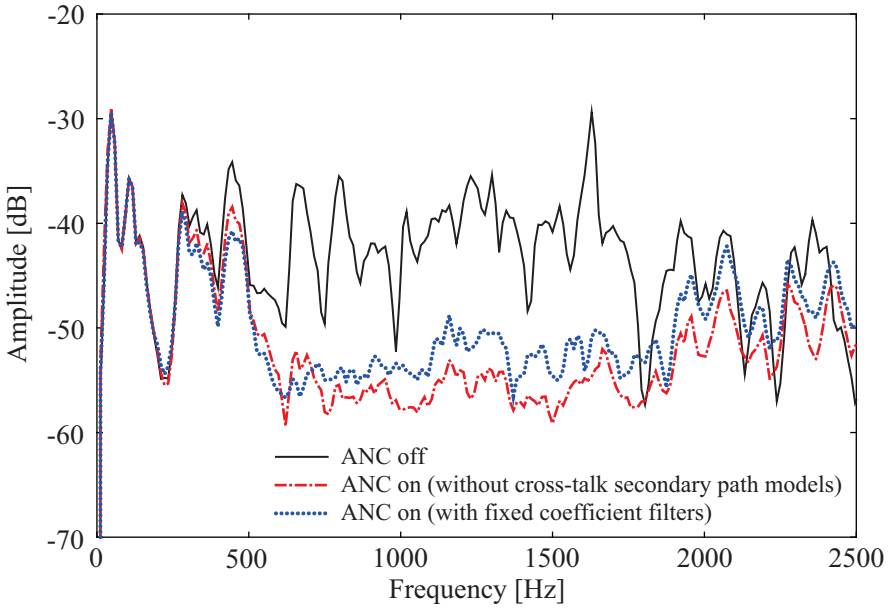

(a) Left ear

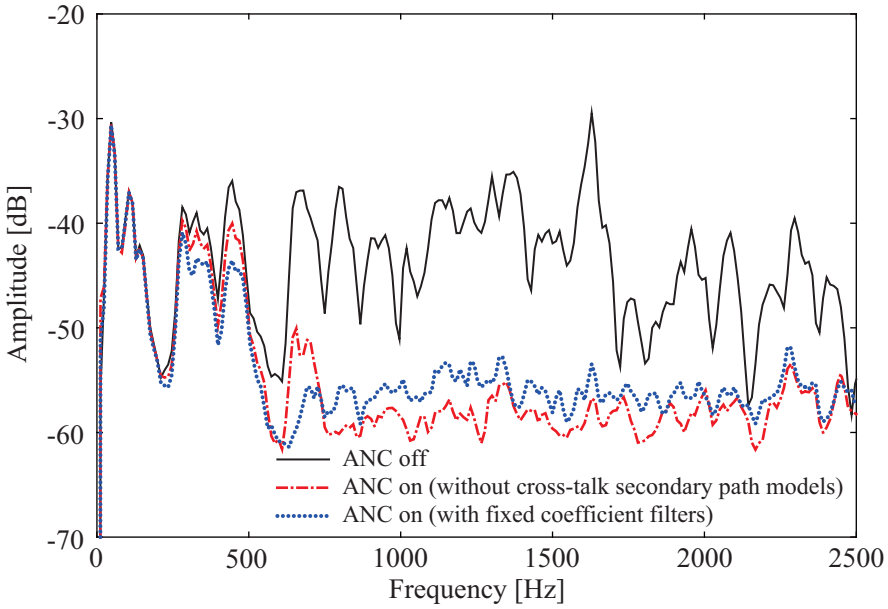

(b) Right ear

Figure 9: Experiment results of the fixed coefficient dual-channel ANC system that achieves 8.0 dB and 12.2 dB noise reductions as compared to the adaptive system achieving 10.5 dB and 13. 7 dB noise reductions at the left and right ears, respectively.

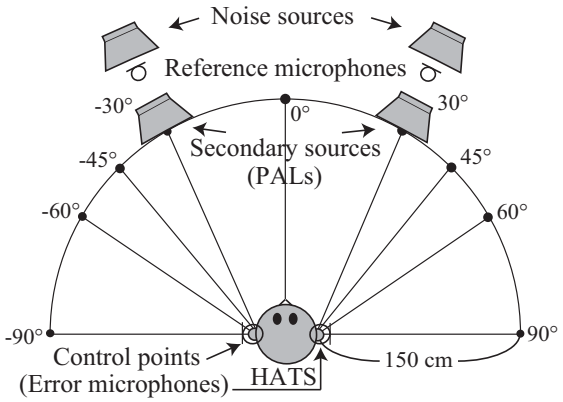

Figure 10: Experimental setup of the dual-channel ANC system when two noise sources are located at $\pm 30°$.

two noise control filters are required in each channel. The structure of the dual-channel ANC system dealing with two noise sources is shown in Fig. 11, where $\mathbf{u}_1(n)$ and $\mathbf{u}_2(n)$ are the reference signal vectors; $d_{11}(n)$, $d_{12}(n)$, $d_{21}(n)$, and $d_{22}(n)$ are the noise signals; $y_{11}(n)$, $y_{12}(n)$, $y_{21}(n)$, and $y_{22}(n)$ are the anti-noise signals.

The normalized FxLMS alogrithm gives the coeffectient update equations of

$$\mathbf{w}_{kj}(n+1) = \mathbf{w}_{kj}(n) + \sum_{m=1}^{2} \frac{\alpha}{\beta + ||\mathbf{x}_{jmk}(n)||^2} \mathbf{x}_{jmk}(n) e_m(n) \tag{8}$$

and

$$\mathbf{w}_{kj}(n+1) = \mathbf{w}_{kj}(n) + \frac{\alpha}{\beta + ||\mathbf{x}_{jkk}(n)||^2} \mathbf{x}_{jkk}(n) e_k(n), \tag{9}$$

when the crosstalk secondary path models are implemented and removed, respectively. In (8) and (9), $j = 1$ or 2 indicates the reference microphone index; $\mathbf{w}_{kj}(n)$ is the updating coefficient vector of the noise control filter; and $\mathbf{x}_{jmk}(n)$ is the filtered reference signal vector. The computational cost of the dual-channel ANC system is further doubled because of the increased

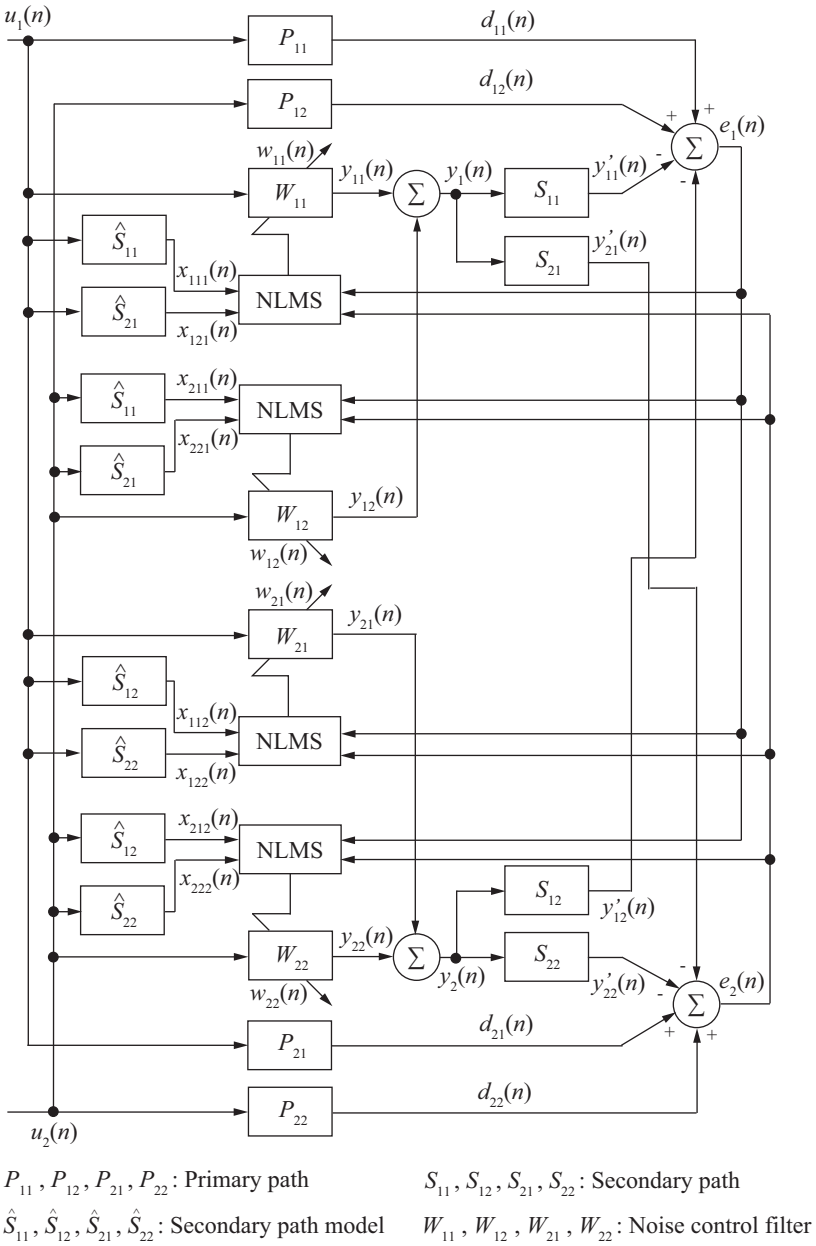

Figure 11: Structure of the dual-channel ANC system using two reference microphones.

number of noise sources, in either case when the crosstalk secondary path models are implemented or removed.

Due to the limitation of the computational capability of the DSP starter kit used in the experiment, the tap length of the noise control filters is reduced to $N = 100$. The rest of the parameters remain the same. The experiment results are shown in Fig. 12. The effective frequency range is not affected, but the noise reduction performance is compromised by the reduced tap length of the noise control filters.

4. Conclusion

In this paper, the binaural ANC system using the PALs as the secondary sources are examined in the application of reducing factory noise. The proposed ANC system creates two quiet zones in the vicinity of the left and right ears of a worker. Considering the narrow directivity of the PAL, the crosstalk secondary path models can be removed to save the computational cost. Based on the experiment results, the dual-channel ANC system outperforms the single-channel ANC system in terms of the effective frequency range and noise reduction performance. The fixed coefficient ANC system demonstrates satisfactory performance with no error microphones placed near the control points. However, when dealing with more than one noise source, the computational cost of the proposed ANC system increases significantly. Therefore, the computational capability of the implementation platform may limit the noise reduction performance, and future improvement is necessary.

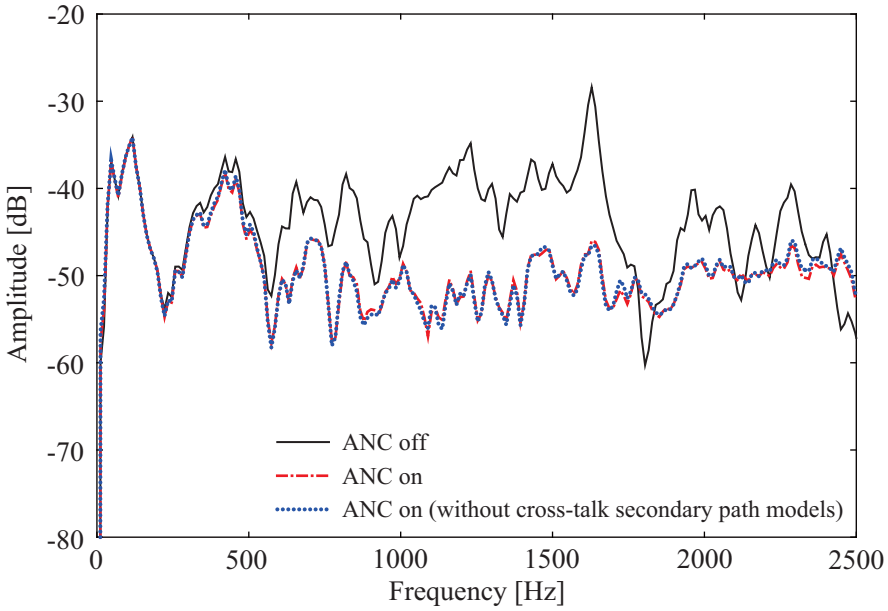

(a) Left ear

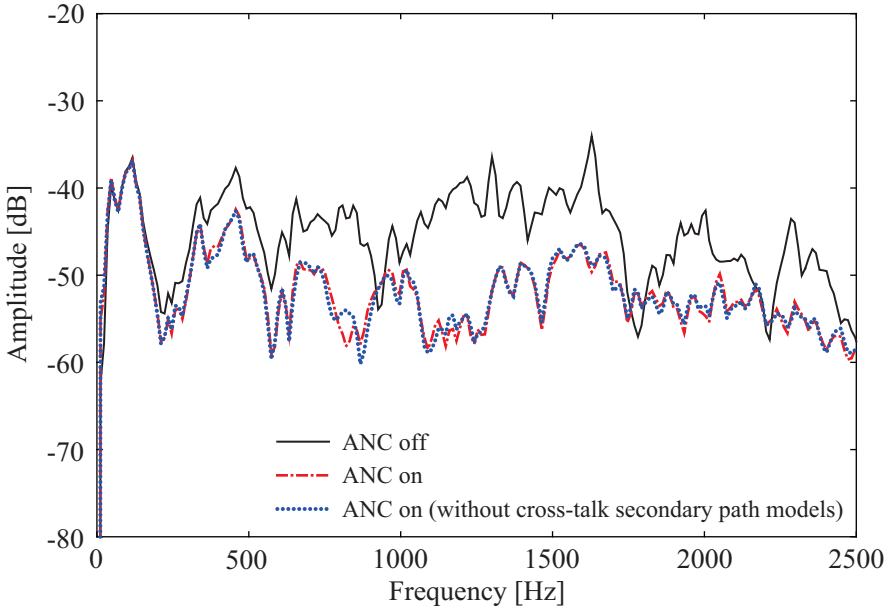

(b) Right ear

Figure 12: Experiment results of the dual-channel ANC system when two noise sources are located at $\pm 30°$. The noise reductions achieved at the left and right ears are 6.8 dB and 7.3 dB, respectively.

5. Acknowledgements

This work is jointly supported by JSPS KAKENHI Grant Number 15K00256 and MEXT-Supported Program for the Strategic Research Foundation at Private University, 2013-2017.

6. References

[1] J. Pan, R. Paurobally, and X. Qiu, "Active noise control in workplaces," *Acoust. Aust.*, DOI:10.1007/s40857-015-0035-2, 1–6 (2015).

[2] S. J. Elliott and P. A. Nelson, "Active noise control," *IEEE Sig. Process. Mag.*, **10**(4), 12–35 (1993).

[3] S. M. Kuo and D. R. Morgan, "Active noise control: a tutorial review," *Proc. IEEE*, **87**(6), 943–973 (1999).

[4] Y. Kajikawa, W. S. Gan, and S. M. Kuo, "Recent advances on active noise control: open issues and innovative applications," *APSIPA Trans. Sig. Inf. Process.*, **1**(e3), 1–21 (2012).

[5] S. J. Elliot, C. C. Boucher, and P. A. Nelson, "The behavior of a multiple channel active control system," *IEEE Trans. Sig. Process.*, **40**(5), 1041–1052 (1992).

[6] S. J. Elliott, I. M. Stothers, and P. A. Nelson, "A multiple error LMS algorithm and its application to the active control of sound and vibration," *IEEE Trans. Acoust. Speech Sig. Process.*, **35**(10), 1423–1434 (1987).

[7] M. Yoneyama, J. Fujimoto, Y. Kawamo, and S. Sasabe, "The audio spotlight: An application of nonlinear interaction of sound waves to a new type of loudspeaker design," *J. Acoust. Soc. Am.*, **73**(5), 1532–1536 (1983).

[8] L. A. Brooks, A. C. Zander, and C. H. Hansen, "Investigation into the feasibility of using a parametric array control source in an active noise control system," *Proc. ACOUSTICS 2005*, Busselton, Australia, 39–45 (2005).

[9] M. R. F. Kinder, C. Petersen, A. C. Zander and C. H. Hansen, "Feasibility study of localised active noise control using an audio spotlight and virtual sensors," *Proc. ACOUSTICS 2006*, Christchurch, New Zealand, 55–61 (2006).

[10] C. Shi, Y. Kajikawa, and W. H. Abdulla, "On adopting parametric array loudspeakers in active noise control," *APSIPA Newslett.*, **1**(10), 6–8 (2015).

[11] T. Komatsuzaki and Y. Iwata, "Active noise control using high-directional parametric loudspeaker," *J. Environ. Eng.*, **6**(1), 140–149 (2011).

[12] B. Lam, W. S. Gan, and C. Shi, "Feasibility of a length-limited parametric source for active noise control applications," *Proc. 21th Int. Congr. Sound Vib.*, Beijing, China, 1–8 (2014).

[13] A. Ganguly, S. H. K. Vemuri, and I. Panahi, "Real-time remote cancellation of multi-tones in an extended acoustic cavity using directional

ultrasonic loudspeaker," *Proc. 40th Annu. Conf. IEEE Ind. Electron. Soc.*, Dallas, Texas, 2445–2451 (2014).

[14] C. Shi, Y. Kajikawa, and W. S. Gan, "An overview of directivity control methods of the parametric array loudspeaker," *APSIPA Trans. Sig. Inf. Process.*, **3**(e20), 1–12 (2015).

[15] R. Tachi and N. Tanaka, "Active noise control using acoustic wave reflection of parametric loudspeaker," *Proc. 13th Asia Pacific Vib. Conf.*, Christchurch, New Zealand, 1–7 (2009).

[16] N. Tanaka and M. Tanaka, "Active noise control using a steerable parametric array loudspeaker," *J. Acoust. Soc. Am.*, **127**(6), 3526–3537 (2010).

[17] N. Tanaka and M. Tanaka, "Mathematically trivial control of sound using a parametric beam focusing source," *J. Acoust. Soc. Am.*, **129**(1), 165–172 (2011).

[18] B. Siravara, M. Mansour, R. Cole, and N. Magotra, "Comparative study of wideband single reference active noise cancellation algorithms on a fixed-point DSP," *Proc. 2013 Int. Conf. Acoust. Speech Sig. Process.*, Hong Kong, **2**, 473–476 (2003)

[19] K. Tanaka, C. Shi, and Y. Kajikawa, "Study on active noise control system using parametric array loudspeakers," *Proc. Forum Acust. 2014*, Krakow, Porland, 1–6 (2014).

[20] K. Tanaka, C. Shi, and Y. Kajikawa, "Multi-channel active noise control using parametric array loudspeakers," *Proc. 2014 APSIPA Annu. Summit Conf.*, Siem Reap, Cambodia, 1–6 (2014).